

The behaviour of iron and aluminium during the diffusion welding of carbon steel to aluminium

M. Kamal Karfoul · Gordon J. Tatlock · Robert T. Murray

Received: 10 November 2005 / Accepted: 31 July 2006 / Published online: 14 April 2007
© Springer Science+Business Media, LLC 2007

Abstract The diffusion welding of carbon steel to aluminium may be achieved when the temperature and compression of the weld metal allows diffusion at the interface between both components; the degree of interdiffusion largely determines the quality of the welded joint. Such diffusion processes can take place under vacuum. However, in this paper, we report that high quality welds can be achieved without the use of vacuum or reducing atmospheres by applying sufficient compression to give very high levels of plastic deformation of an Al layer sandwiched between layers of carbon steel at 550 °C in laboratory air. The resulting structures were characterised using scanning electron microscopy, transmission electron microscopy and microanalysis, which showed that, under these conditions, Fe diffused across the interface into the Al layer.

Introduction

It is known that the diffusion welding (DW) of carbon steel (CS) with aluminium can only be achieved with extreme difficulty because of the large difference in physical and

chemical properties between the two metallic components. During this process, potentially deleterious intermetallic phases such as FeAl_3 , Fe_2Al_7 , Fe_2Al_5 , FeAl_2 can precipitate in the weld zone [1]. When these precipitates grow to the point where a complete layer of significant thickness is formed, the joint becomes too brittle and the weld is effectively destroyed. To avoid the formation of brittle phases at the interface, the use of an intermediate layer of nickel has been proposed [1]. Alternatively, a joint may be formed by brazing, using a Si–Al eutectic [1, 2]. However, DW of steel with Al may be achieved directly when the temperature and compression of the weld promotes the diffusion at the interface between both halves of the joint, and the degree of interdiffusion largely determines the quality of the weld. Such diffusion processes have only previously been demonstrated under vacuum or in reducing atmospheres.

To achieve a good diffusion weld of stainless steel (SS) with Al, it is enough to use heat treatment plus compression to give high plastic deformation of the Al layer without using either vacuum or reducing atmospheres as a protection from air oxidation [3, 4]. Of course, the DW process should be accomplished at temperatures less than the melting point of Al (i.e., less than 660 °C). At this temperature, Al oxide (Al_2O_3) will not dissociate in air and, therefore, it is expected to be present at the interface between the welded metals (SS and Al). In theory, welding should not then take place, but in practice it was proved [3] that DW joints could be achieved under normal atmospheric conditions without the use of vacuum or reducing atmospheres, and it appears that the Al oxide does not prevent DW.

Data about the dispersion of active metal oxides (like Al oxide) on the surface of their parent metals at high temperatures are not plentiful, although there is some data

M. K. Karfoul (✉)
Faculty of Chemical & Petroleum Engineering, Al-Baath
University, P.O. Box 1173, Homs, Syria
e-mail: karfoulmk@yahoo.co.uk

G. J. Tatlock · R. T. Murray
Department of Engineering, Materials Science, The University
of Liverpool, Liverpool L69 3GH, UK

G. J. Tatlock
e-mail: g.j.tatlock@liverpool.ac.uk

concerning aluminium and titanium oxides [5, 6]. In [6], for example, it is reported that thinning of titanium oxide may occur under vacuum when heated within the temperature range from 525 to 625 °C. However, since the DW of Al with SS has been reported as taking place under ambient atmospheres [3], it is clear that the Al oxide must not remain at the Fe/Al interface as a continuous film. It has also been shown that very high levels of plastic deformation give an improved weld [7]. Compression during welding probably has a positive effect on the diffusion process by dispersing the Al oxide layer, which may be further disrupted if plastic deformation is used. Hence further analysis at high spatial resolution could give new insight into the process, which could be of real importance if DW under ambient atmospheres can be routinely achieved.

Welding procedure

A36 carbon steel plate of composition C = 0.24 wt.%, Mn = 0.7 wt.%, Si = 0.3 wt.%, P = 0.04 wt.%, S = 0.05 wt.% and thickness 1.50 mm, was used for the experiments together with aluminium foil type 1100 of thickness 0.020 mm. The samples were prepared from cut pieces measuring 8 × 58 mm from both materials. The faces of the steel were ground on 600 grit SiC paper until they became free of any deposits and then washed with detergent and water. The roughness of steel plates surface R_z was 0.9 μm . The plates were then combined with Al foils under ethanol to ensure that no further surface contamination was introduced. The final sample sandwich structure is illustrated in Fig. 1.

This metallic sandwich was carefully loaded under compression in a special test rig, which incorporated electric heating of the work piece. The maximum load capacity available was 10,000 kgf. The sample was first compressed to 0.2 MPa, then heated to 550 °C. While still at this temperature, the load was increased to 2 MPa for 15 min. Then the sandwich was unloaded and removed from

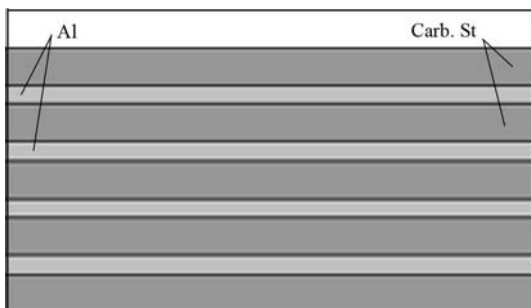


Fig. 1 The sandwich sample

the testing machine for further studies. All samples were stored in a closed, dry atmosphere. Specimens were prepared from the sandwich-samples for studying by light, scanning (SEM), and transmission (TEM) electron microscopy. The SEM used was a *Hitachi S-2460N* at a voltage of 25 kV. The TEM was a *JEOL - 2000 FX II* at 200 kV. EDX analysis was carried out on both the TEM and SEM.

Experimental results and discussion

Cross-section specimens, cut from the DW sample, showed that, after compression, the thickness of the Al layer was reduced from 20 μm to about 10 μm (Fig. 2). The selected period of diffusion (15 min) allowed a very limited amount of interdiffusion. Hence it was necessary to study the diffusion couple at high spatial resolution on both sides of the interface between the steel and the aluminium. Specimens were prepared by polishing and/or ion beam thinning and studied in both the SEM and TEM.

The interface

Figure 3 shows a transmission image across the interface area after welding. The diffraction patterns (Figs. 4, 5) from areas close to the interface show a characteristic body centred cubic (bcc) lattice on the steel side and a face centred cubic (fcc) lattice on the Al side of the interface, as expected.

EDX spectral analysis performed on the steel area close to the interface (Fig. 6) clearly shows that the Al content is below the minimum level of detection in the TEM. Practically, this means that there is effectively no diffusion of Al into the iron, whereas, on the other side of the interface (the Al side) the EDX spectrum (Fig. 7) shows that there is a substantial content of iron inside the Al at a point about 0.1 μm from the interface. Hence the Fe has crossed the interface and diffused into the Al layer. EDX analyses were also carried out at a point on the Al side of Fe/Al interface

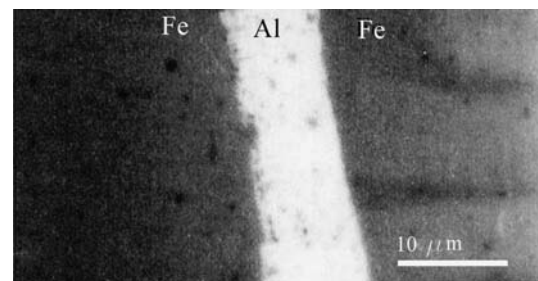


Fig. 2 The reflected light image of a sandwich section. The aluminium layer thickness is about 10–15 μm after welding as a result of the high plastic compression

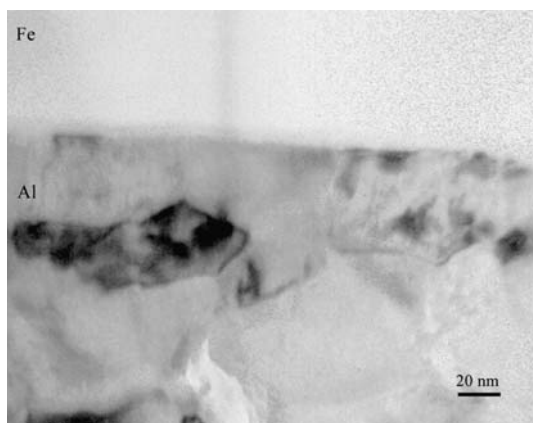


Fig. 3 TEM image of a welded zone near the Fe/Al interface

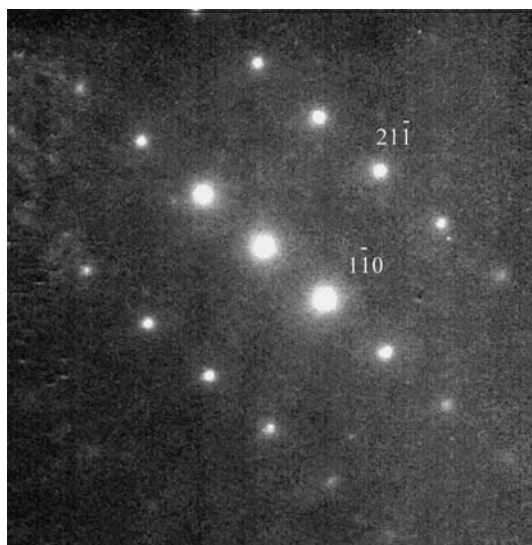


Fig. 4 Diffraction pattern from the Fe area close to the Fe/Al interface, $\langle 113 \rangle$ bcc lattice

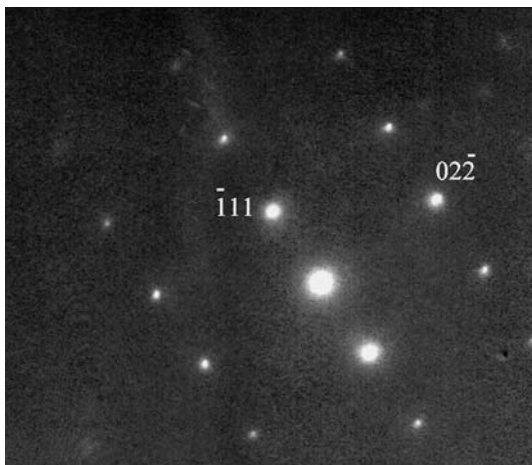


Fig. 5 Diffraction pattern from the Al area close to the Fe/Al interface, $\langle 211 \rangle$ fcc lattice

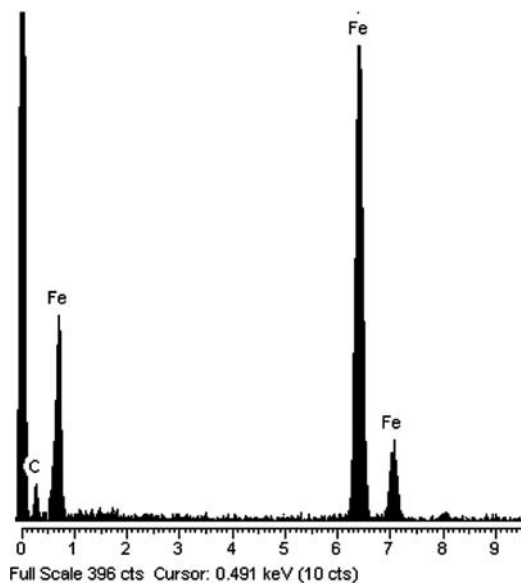


Fig. 6 EDX from the steel area 100 nm from the Fe/Al interface

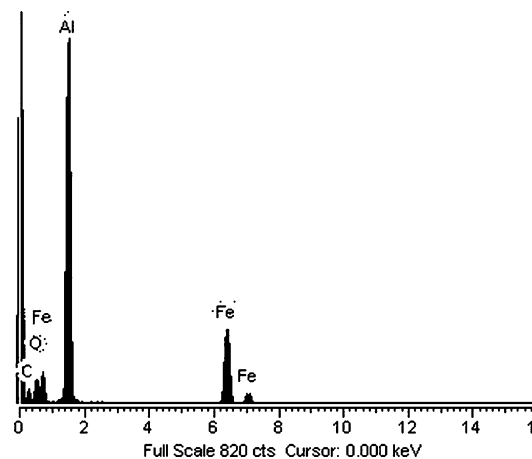
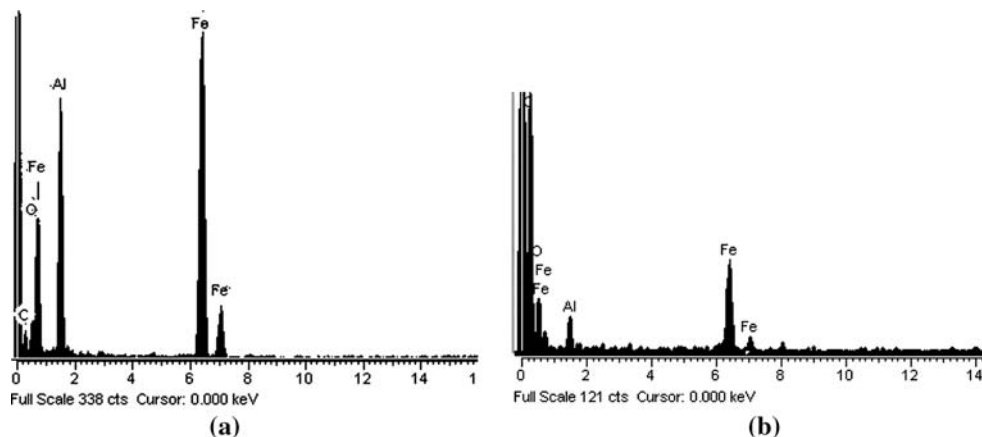


Fig. 7 EDX from the Al area 100 nm from the Fe/Al interface

and at the interface itself (Fig. 8). These analyses show that the Al-concentration close to the interface is about 40 at.% and the Fe-concentration is about 60 at.%, while other EDX analyses at points along the Fe/Al interface show that the Fe concentration here is about 75 at.%. Thus, it can be considered that the interface phase lies between Fe_3Al and FeAl intermetallic phases. The Fe atoms diffuse inside the Al layer until, at the composition corresponding to Fe_3Al , there is a stoichiometric arrangement [8]. Further into the Al layer, the FeAl intermetallic phase is preferred. EDX analysis from a spot size about 50 nm therefore gives an intermediate composition between the intermetallic phases. At a spot 0.5 μm from the Al side of the Fe/Al interface, the EDX analysis shows that the Fe content is still greater than 3.00 at.%. In an attempt to verify this, the lattice parameter was also measured. With the sample mounted in

Fig. 8 EDX spectra from points near the CS/ Al interface: (a) Al side of Fe/Al interface, (b) at the Fe/Al interface



holder position 1 of a side entry double tilt holder in the JEOL 2000FX, a thin evaporated film of fine-grained Al was mounted in position 2. Care was taken to adjust the eucentric height and astigmatism, and focus on the selected area aperture, before recording the diffraction patterns from the two samples, although a small error could be introduced on movement between the two samples. The DP from the $\langle 112 \rangle$ zone axis on the Al side of the interface (Fig. 9) was then compared with the ring patterns from the fine grained standard (Fig. 10). The overall average parameter ratio of standard lattice to the measured lattice was 1.032 ± 0.005 . Thus the lattice deformation caused by Fe diffusion may be as high as $3.0 \pm 0.5\%$, compatible with an Fe content of $>3\%$ measured by EDX (Fig. 11). The variation in Fe content in the Al-containing areas close to the interface is demonstrated by the data in Fig. 12. In this case, it is clear that the diffusion is from the steel layer to the Al layer, and that the iron atoms cross the CS/Al interface into the Al layer. At the reaction temperature, different intermetallic phases such as Fe_3Al and/or FeAl

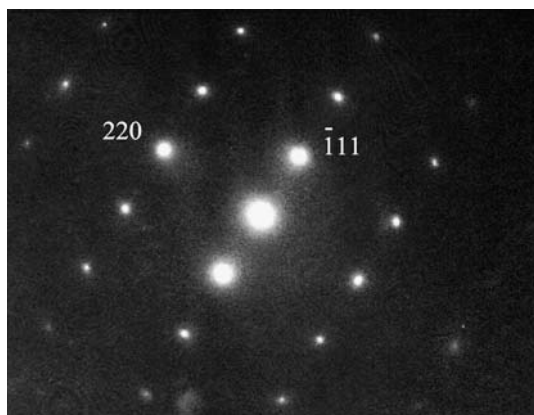


Fig. 9 Diffraction pattern from a spot $0.5 \mu\text{m}$ from the Fe/Al interface on the Al side, $\langle 211 \rangle$ fcc lattice

may be formed. As the Fe content falls across the Al layer, it is probable that another intermetallic phase, such as FeAl_3 , forms because, thermodynamically, this phase is the most stable when the Fe content is between 0.9 and 24 at.% (as shown in the Fe–Al phase diagram [9]). The result of EDX analyses in regions $0.2 \mu\text{m}$ into the Al layer shows that Fe content here is about 20 at.%.

The Fe concentration as a function of the diffusion depth is shown in Fig. 12. Two zones may be identified. The first, zone 1, contains the Fe_3Al and FeAl phases, with the Fe concentration (C) related to the diffusion depth x by some function $C = f(x)$. The initial Fe concentration C_s should be 75 at.% at the edge of the zone, dropping to $C_1 = 55$ at.% as zone 2 is entered. In this second zone FeAl_2 , Fe_2Al_5 and FeAl_3 may be present and the zone should cover the region until $C_2 = 25$ at.%. In fact, this band continues out to a distance of $1 \mu\text{m}$, with a smooth decrease in the Fe content. This may be due to the presence of varying amounts of the eutectic within the aluminium.

To model the formation of this complex system, only two zones, with two diffusion coefficients were assigned: D_1 —iron diffusion coefficient in Fe_3Al rich phase zone and D_2 —iron diffusion coefficient in FeAl_3 rich phase zone, with $D_1/D_2 = \varphi$. If one of these coefficients is known, the other can be determined. Thus the Fe atomic fraction in Al (c) at a distance ζ from the interface position ($x = 0$) has the values corresponding to Fe_3Al rich phase zone, while the Fe flows across the Matano interface and produces an FeAl_3 rich phase zone. Therefore this model of Fe diffusion may be described by the change of the Matano interface position with time (t). To derive the diffusion coefficients D_1 and D_2 the method of Seith [10] based on Fick’s second law and the Kirkendall effect was applied to diffusion in the multiphase solid system. For diffusion time $t > 0$, the equation of Fick’s law takes the following form:

$$\frac{\partial C}{\partial t} = D_2 \frac{\partial^2 C}{\partial x^2} \quad \zeta < x < \infty, \tag{1}$$

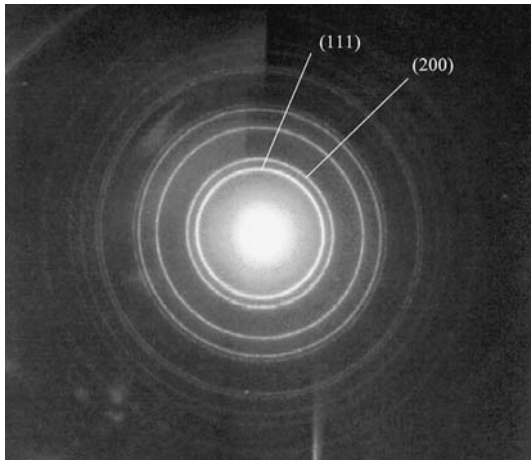


Fig. 10 Ring diffraction pattern of fine grained standard Al

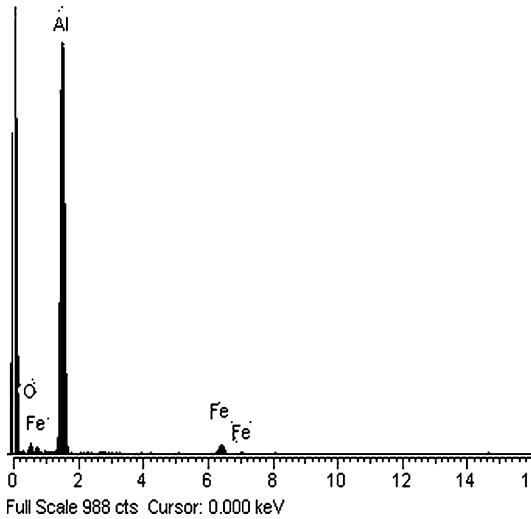


Fig. 11 EDX analysis from a point 0.5 μm from the Fe/Al interface. The Fe content is about 3.0%

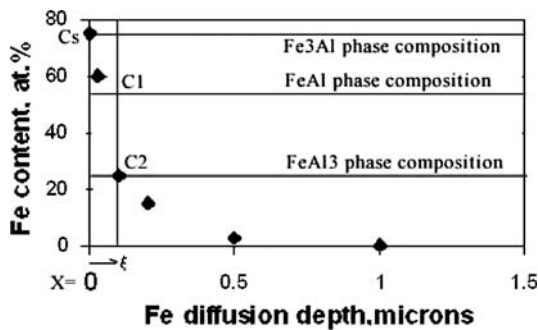


Fig. 12 Fe content (at.%) in the Al area close to the Fe/Al interface

$$\frac{\partial C}{\partial t} = D_1 \frac{\partial^2 C}{\partial x^2} \quad 0 < x < \zeta. \tag{2}$$

The general solutions of Fick’s equations 1 and 2 are:

$$C = C_s - B_1 \psi\left(\frac{x}{2\sqrt{D_1 t}}\right), \tag{3}$$

$$C = C_2 - B_2 \psi\left(\frac{x}{2\sqrt{D_2 t}}\right), \tag{4}$$

where B_1 and B_2 are constants, $\psi(x/2\sqrt{Dt})$ is an error function of argument $x/2\sqrt{Dt}$.

Co-ordinate $x = \zeta$ corresponds to the Matano position, given by

$$\zeta = 2b\sqrt{D_1 t}, \tag{5}$$

where b is a constant.

For the initial condition $t = 0, C = C_0 = 0$, and boundary conditions:

For Fe_3Al phase : at $x = 0$,
 $C = C_s = 75\%$, and at $x = \zeta, C = C_1$,
 $B_1 = \frac{C_s - C_1}{\psi(b)}. \tag{6}$

For $FeAl_3$ phase : at $x = \zeta, C = C_2, B_2 = \frac{C_2 - C_0}{\psi(b_2)}, \tag{7}$

where

$$b_2 = b\sqrt{\varphi}, \tag{8}$$

and at

$$x = \infty, C = C_0. \tag{9}$$

C_0 is the initial Fe concentration inside the Al layer which in this case should be almost zero.

The mass balance equation at the boundary between Fe_3Al and $FeAl_3$ rich zones takes the following form:

$$(C_1 - C_2) \frac{d\zeta}{dt} = -D_1 \left(\frac{\partial C}{\partial x}\right)_{C_1} + D_2 \left(\frac{\partial C}{\partial x}\right)_{C_2}. \tag{10}$$

Hence for $\zeta = x$

$$C_1 - C_2 = \frac{C_s - C_1}{\sqrt{\pi b e^{b^2}} \psi(b)} - \frac{C_2 - C_0}{\sqrt{\pi b \sqrt{\varphi} e^{b^2 \varphi}} \psi(b\sqrt{\varphi})}. \tag{11}$$

The value of φ can be computed from Eq. 11.

Therefore, when $b = 0.37, \varphi = 1.6, x = 0.1 \times 10^{-4}$ cm, then $D_1 = 2 \times 10^{-13}$ cm²/s and $D_2 = 1.3 \times 10^{-13}$ cm²/s,

which are high enough to achieve a DW after 15 min at 550 °C.

The break up of the protective Al₂O₃ scale on the aluminium layers, may be promoted by the roughness of the steel surfaces. Following Schutze [11], we assume that buckling precedes through-thickness cracking of the scale. Hence to promote cracking, the critical strain for buckling needs to have been exceeded. The critical strain for buckling ϵ_c takes the form [11]:

$$\epsilon_c = \frac{1.22}{1 - \nu^2} \left[\frac{d}{R} \right]^2, \tag{12}$$

where d = scale thickness, R = the initial bend radius of the substrate on which the scale is supported ($R = Rz$), and ν = Poisson’s ratio (≈ 0.24 for alumina). At 550 °C the thermal strain is 10^{-2} and for a growth time of 15 min at 550 °C the oxide thickness is about 17.5 nm [5]. Thus R required to give decohesion is 0.2 μm , which is likely to be exceeded unless the steel is polished or ground very finely. Therefore it can be assumed that the Fe diffusion can proceed across the interface when the surface interface roughness is greater than R . The dispersion of the oxide layer speeds up the Fe diffusion across the Fe/Al interface, and fragments of oxide may be observed in Fig. 13. This is also consistent with the high oxygen signals present in the spectra shown in Figs. 7, 8.

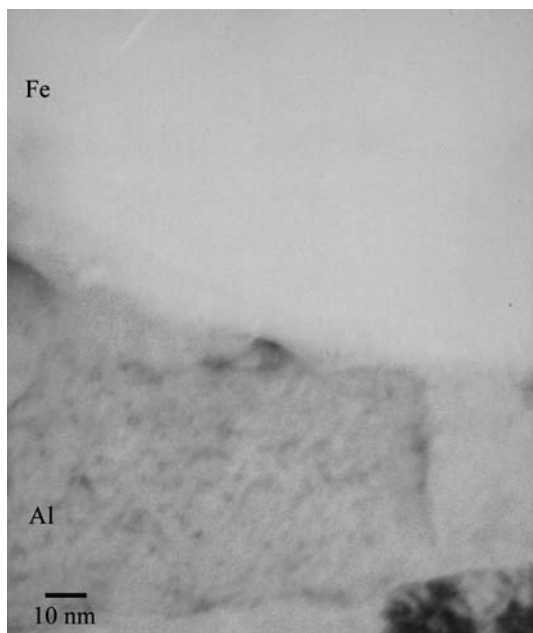


Fig. 13 A higher magnification TEM image of the Fe/Al interface shown in Fig. 3

Heat treatment at 640 °C

To study the influence of heat treatment close to the melting point of pure Al (660 °C) in the DW sandwich, specimens were subjected to air exposure in an electric oven for 72 h at 640 ± 2 °C. Figure 14 shows the SEM image of a diffused weld in which four spots mark the points where EDX analyses were carried out. Figures 15, 16, 17, 18 show the results of these analyses, which indicate that Fe has now diffused deeply into the Al layer (Figs. 16, 17). The Fe levels in the aluminium layer are high but the aluminium content of the iron layer remains very low, suggesting that the aluminium cannot diffuse far into the steel, at this temperature. Similar results have been reported for DW of SS with Al [3] and titanium with Al [12, 13]. It has been reported that inert marker experiments using tungsten markers indicated net movement of Fe or Ti into Al for both SS and titanium alloys [3, 4, 13]. But Luo and Acoff [12] using electron microscopy and micro hardness testing, found that the titanium had diffused inside the Al at temperatures around the melting point of the Al. In the present case, the Fe diffusion into the Al layer produced intermetallic phases: for spots 2 and 3 on Fig. 14, 40 at.% Fe and 60 at.% Al. These are consistent with a phase composition of FeAl₂. By using the model discussed in the previous section for calculation of the Fe diffusion coefficient in an Al layer, values of $b = 0.22$ and $\varphi = 1.044$, $D_1 = 7.2 \times 10^{-13} \text{ cm}^2/\text{s}$ and $D_2 = 6.9 \times 10^{-13} \text{ cm}^2/\text{s}$ were derived.

Such heat treatment, applied to a DW sample after welding, has the advantage of producing Fe–Al alloy in the aluminium layer which has a melting point higher than that of pure Al as shown in the Fe–Al phase diagram [9]. Hence subsequent heat treatments can be carried out at temperatures higher than 660 °C without any danger of melting the aluminium layer.

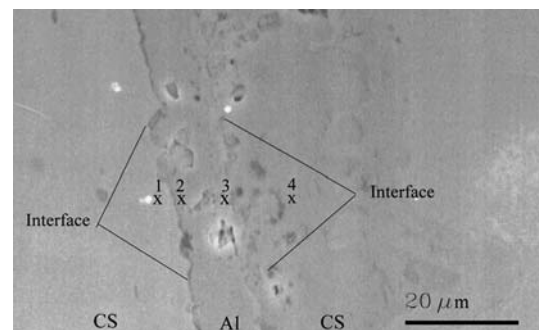


Fig. 14 SEM image showing the locations of points from which EDX spectra were collected after heat treatment at 640°C for 72 h

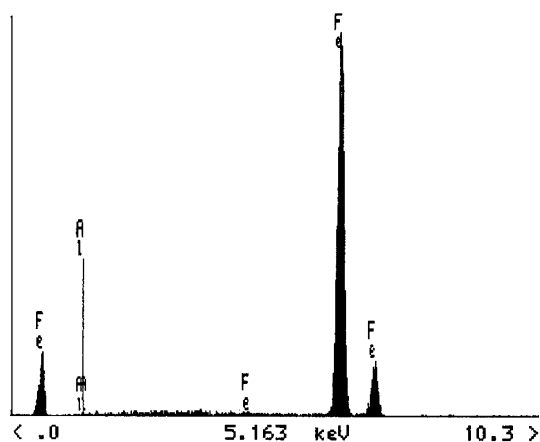


Fig. 15 EDX spectrum from spot 1 in Fig. 14

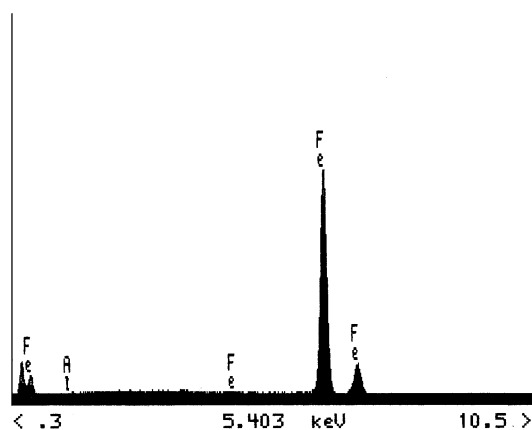


Fig. 18 EDX spectrum from spot 4 in Fig. 14

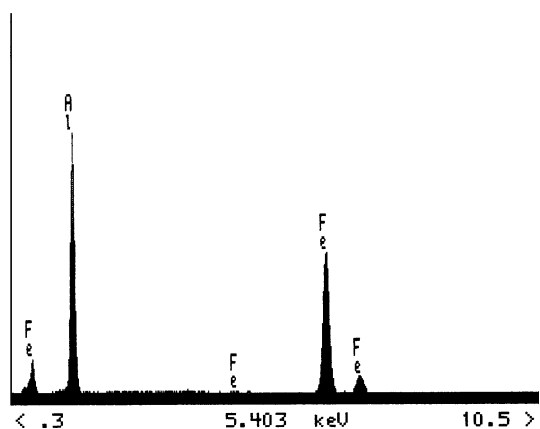


Fig. 16 EDX spectrum from spot 2 in Fig. 14

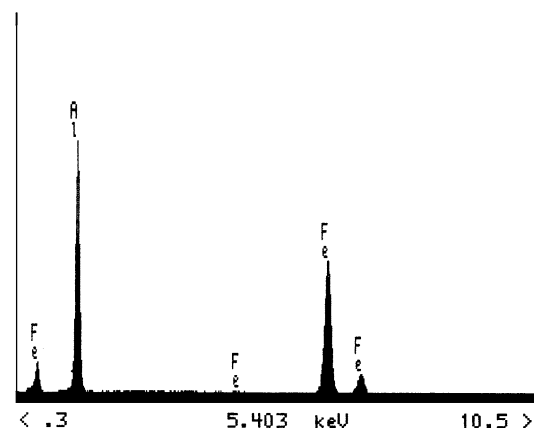


Fig. 17 EDX spectrum from spot 3 in Fig. 14

Conclusions

- (1) This study illustrates the feasibility of diffusion welding carbon steel to Al under ambient conditions, without the use of a vacuum. The only necessary

conditions for the successful welding operation were the use of plastic deformation of the welded sandwich between layers of ordinary carbon steel with a moderate surface finish. Such treatment appeared to divide the continuous Al oxide film on the Al surface layer into small pieces, and showed that this oxide film did not greatly inhibit the subsequent diffusion process at the carbon steel/Al interface.

- (2) At welding temperatures below the melting point of Al, the Fe diffused inside the Al layer of the welded sandwich and formed Fe–Al alloys that have melting points higher than the Al melting point, whereas, there was no detectable Al diffusion inside the steel layer at these temperatures.
- (3) During the diffusion welding process of the carbon steel A 36 to Al 1100 at 550 °C and plastic deformation for 15 min, an iron rich alloy was formed at the interface, and FeAl₃ intermetallic phase was probably formed at distances greater than 0.1 μm within the Al.
- (4) Heat treatment of the welded composite at 640 °C for 72 h produced a composition close to FeAl₂ throughout the Al rich layer.

Acknowledgements This work was carried out in the Materials Laboratories in Department of Engineering at the University of Liverpool, UK. The authors thank the staff of these laboratories for their cooperation in the completion of this work.

References

1. Kazakov NF (1976) Diffuzionnaia Svarka Materialov. Mashinostroenie, Moscow, p 58
2. Roulin M, Luster JW, Karadeniz G, Mortensen A (1999) Welding J 78(5):155-s
3. Karfoul MK, Hamed H (2003) Bassel al-Asad J Eng Sci (17):67

4. Karfoul MK, Hamed H (2004) In: Proceedings of International Mechanical Engineering Conference (IMEC) 2004, Kuwait, pp 636–646
5. Benard J (1962) Oxidation Des Metaux (Russian Translation) (1968), V.II, p 311
6. Bondar AV, Peshkov VV, Kireev LS, Shurourov VV (1998) Diffusionnaia Svarka Titana i ego Splavov. The University of Voronej, Russia, p 46
7. Yeh MS, Tseng YH, Chluang TH (1999) Welding J (AWS) 78(Sept.):301-s
8. Bradley AJ, Jay AH (1934) Proc Roy Soc A 136:211
9. Kubasschewski O (1982) Iron – binary phase diagrams. Springer-Verlage, Berlin, pp 5–9
10. Seith W (1955) Diffusion in metallen. Springer-Verlag, Berlin, Rus. Issue, 1958, p 202
11. Schutze M (1995) Oxid Metals 44(1–2):29
12. Luo J-G, Acoff VL (2000) Welding J (AWS) 79(9):239-s
13. Karfoul MK, Hamed H (2003) Bassel al-Asad J Eng Sci 18:71